

Supporting information

Correlation of electrochemical and ab initio investigations of Iron poly-bipyridine coordination complexes for battery applications: impact of anionic environment and local geometries of the redox complexes on the electrochemical response

Adama Sy,[§] Asif Iqbal Bhatti,[‡] Fahim Hamidouche,[†] Olivier Le Bacq,[‡] Lauréline Lecarme,[†] Jean-Claude Leprêtre^{†,□}

[§] Univ. Gaston Berger, UFR SAT, Saint – Louis, 32002, Senegal

[†] Univ. Grenoble Alpes, Univ. Savoie Mont Blanc, CNRS, Grenoble INP, LEPMI, 38000 Grenoble, France

[‡] Univ. Grenoble Alpes, CNRS, Grenoble INP, SIMAP, 38000 Grenoble, France

* E-mail: Jean-Claude.Lepretre@lepmi.grenoble-inp.fr Jean-Claude.Lepretre@lepmi.grenoble-inp.fr

TABLE OF CONTENTS

- **Supplementary complexes characterizations**

Figure S1. ^1H NMR of the $\text{Fe}(\text{DmbPy})_3(\text{ClO}_4)_2$ complex.

Figure S2. ^1H NMR of BisbPy ligand.

Figure S3. ^1H NMR of the $\text{Fe}_2(\text{BisbPy})_3(\text{ClO}_4)_4$ complex.

Figure S4. UV-visible spectra of mono and bi nuclear Iron complexes.

- **Settings of the ab-initio calculations**

- **Calculated interatomic distances**

Table S.1. Selected calculated bond lengths for $[\text{M}(\text{bPy})_3]^{2+}$ and $[\text{M}(\text{bPy})_3]^{3+}$ complex when considered alone and in the field created by the PF_6^- counter-ions.

Table S.2. Selected calculated bond lengths for $[\text{M}(\text{bPy})_3]^{2+}$ and $[\text{M}(\text{bPy})_3]^{3+}$ complex in the field created by the ClO_4^- , PF_6^- and TFSI^- counter-ions.

- **Supplementary references**

- Supplementary complexes characterizations

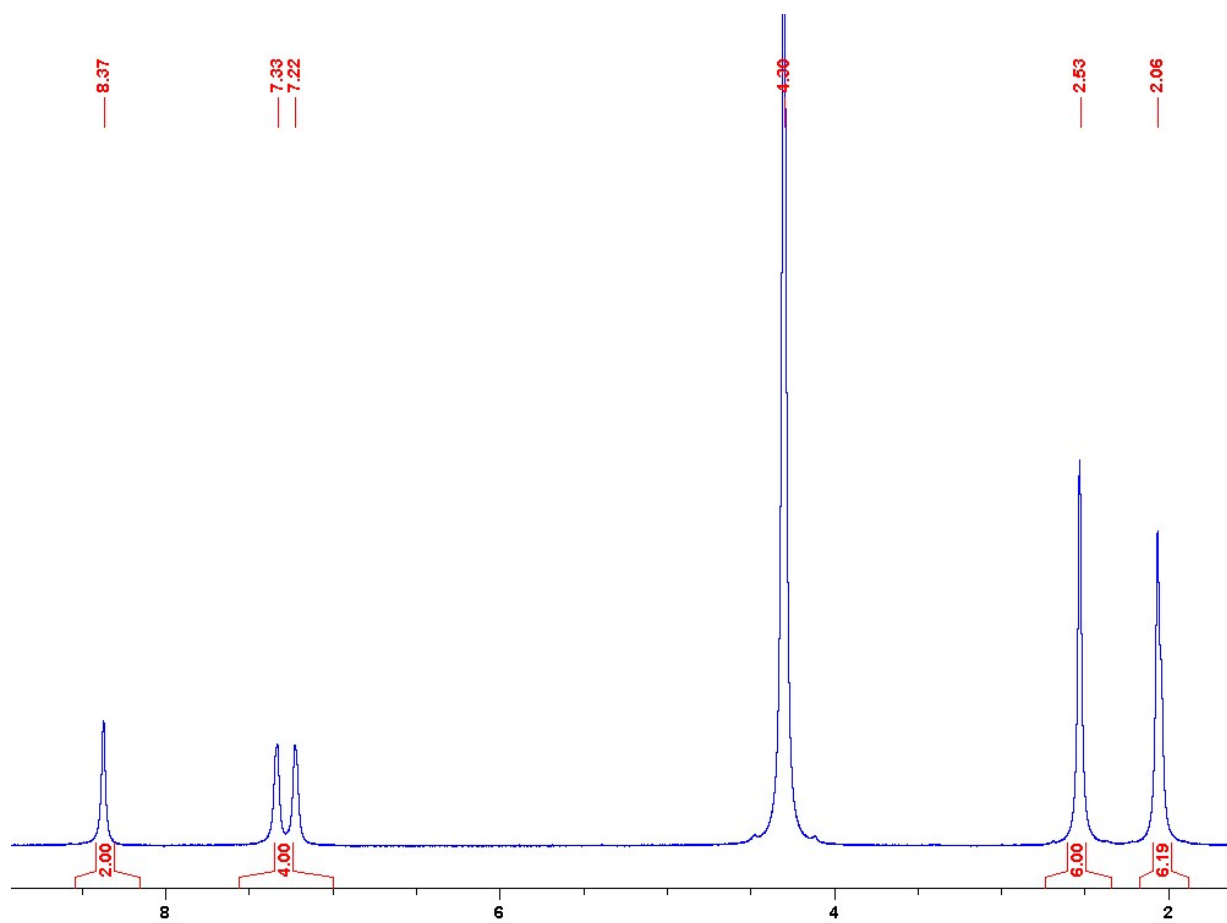


Figure S1. ¹H NMR of the Fe(DmbPy)₃(ClO₄)₂ complex in CD₃NO₂.

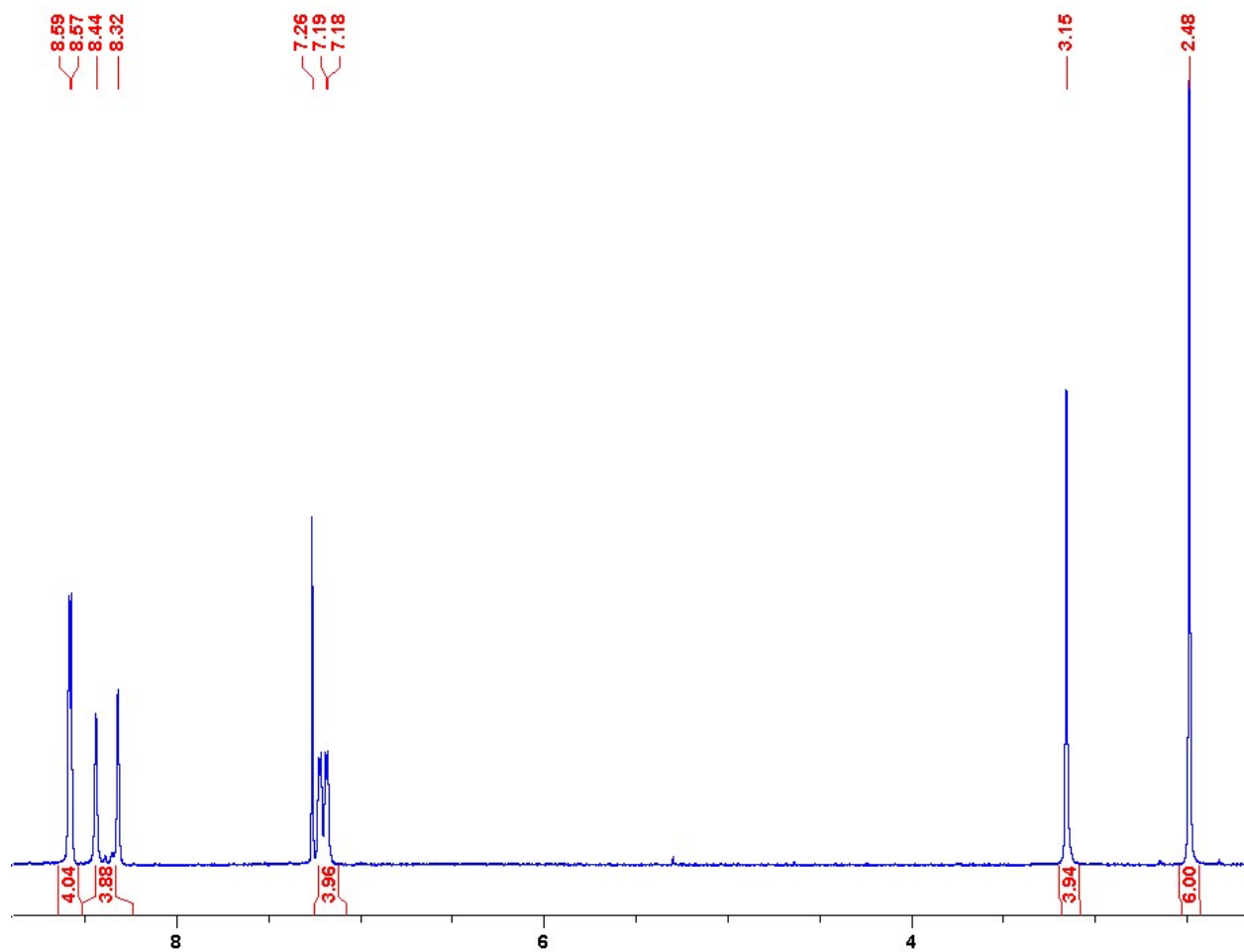


Figure S2. ¹H NMR of BisbPy ligand in CD₃Cl.

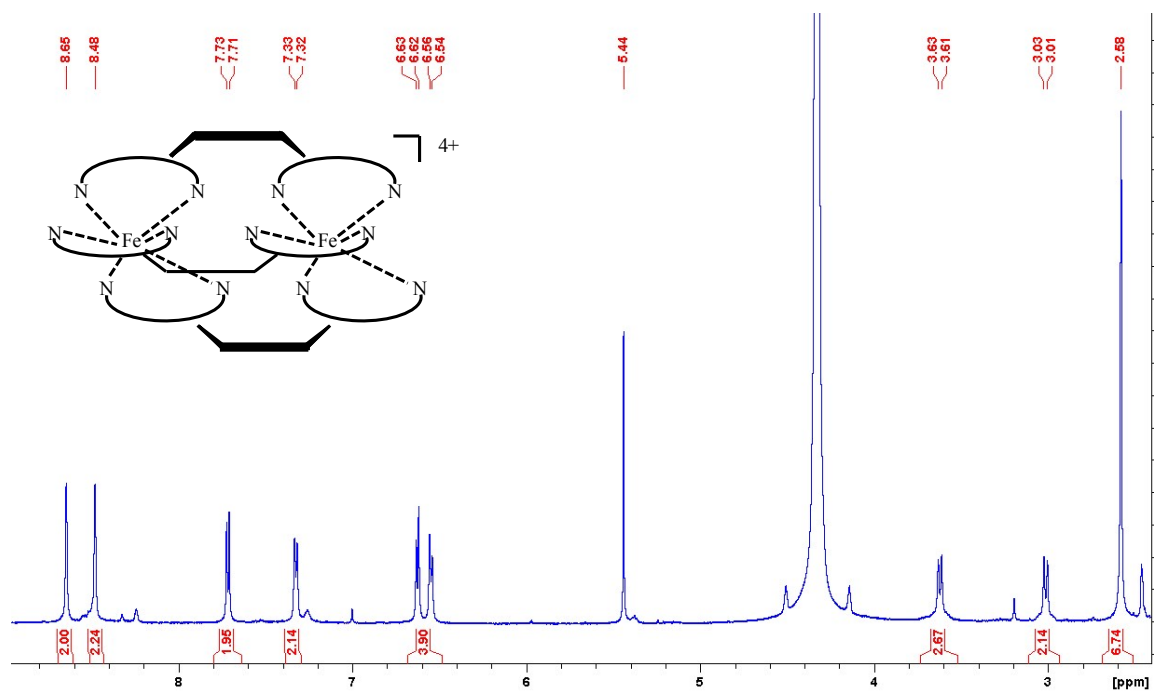


Figure S3. ^1H NMR of the $\text{Fe}_2(\text{BisbPy})_3(\text{ClO}_4)_4$ complex in CD_3NO_2 .

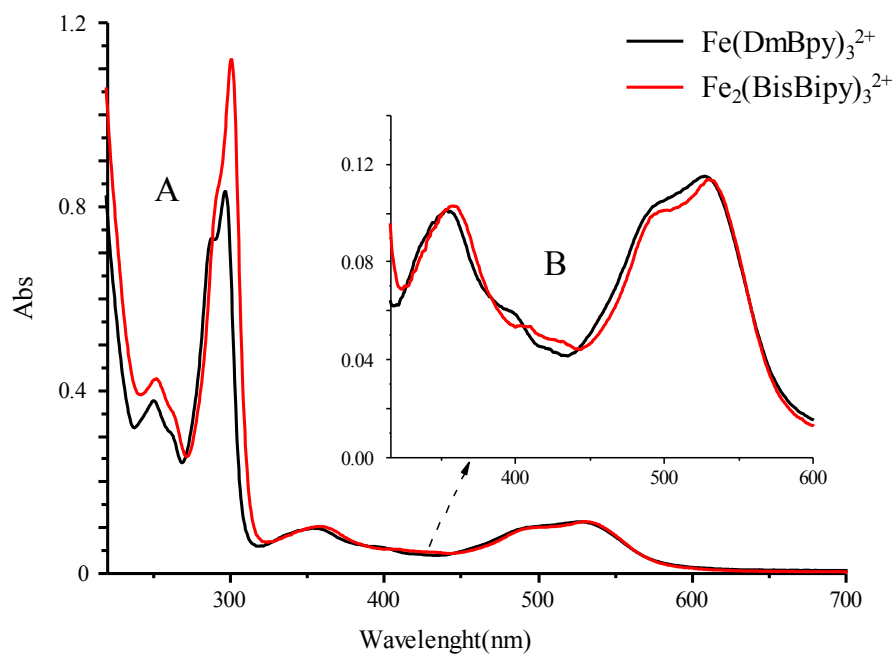


Figure S4. UV-visible spectra of mono and bi nuclear Iron complexes in CH_3CN , $[\text{Fe}] = 0.13 \text{ mM}$, $l = 1 \text{ mm}$.

- **Details of the ab-initio calculations**

All calculations were performed using Gaussian09 program¹. This code relying on the Density Functional Theory² uses an all-electron basis sets. The basis set of Aldrich^{3,4} in both Def2-SVP and Def2-TZVP formulations were considered. The calculated voltages as well as the relaxed atomic positions were actually found insensitive to the choice of the basis and the calculations presented in the present work use the Def2-SVP basis. Symmetries were switch off in all our calculations, allowing the systems to adopt the optimized geometry without being restricted by the symmetry of the initial conformation. The geometries were considered as converged when the forces on every atom were lower than $1 \cdot 10^{-5}$ Hartree/Bohr. In all the calculations, ultrafine grid was used for numerical integration in reciprocal space.

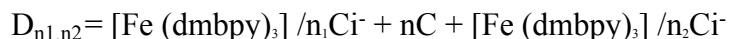
Various exchange and correlation functionals were investigated. Among the most relevant (regarding their ability to capture the thermodynamics and structural properties of our compounds), PBE⁵ and PBE0⁶ functionals (with, for this latter, a 25% Hartree-Fock factor for the exchange contribution) were finally selected. Here, we will only provide our results based upon the PBE approximation, for which a very clear description of the electronic structure is obtained, namely, a recovery of the ligand field theory with the neat appearance of e_g and t_{2g} levels, as expected for an octahedral environment of ligands all around a transition metal atom. If the PBE0 approximation leads to very similar structural properties compared to PBE approximation (so that it does not bring any further essential information for our inquiry), the electronic structure remains more problematic to be interpreted and deserves a more specific study.

To conclude on this technical part, let us mention that our calculations were performed for the various possible $2S+1$ spin multiplicities in order to determine the absolute magnetic ground state. For open-shell systems, unrestricted spin formalism was used. For $[\text{Fe}(\text{DmbPy})_3]^{2+}/2\text{Ci}^-$ (*case of Fe II*), the ground state was found to be singlet in agreement with independent experimental and DFT calculations⁷. For full loaded system, $[\text{Fe}(\text{DmbPy})_3]^{3+}/3\text{Ci}^-$, the lowest spin multiplicity was found to be the doublet as expected in references^{7,8}.

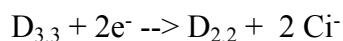
- **Calculation of the voltage of the dimers**

The voltages for the bi-nuclear compounds were derived by generalizing the expression for mono-nuclear potential. The expression for the dimer is:

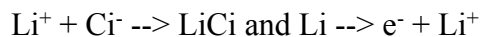
The dimer is made of two mono-nuclear patterns connected by an alkyl chain. Let's denote $n\text{C} \equiv -(\text{CH}_2)_n-$ the alkyl chain used as the linker. Ci^- labels the counter-ions surrounding each active center. n_1 counter-ions surround the first monomer and n_2 counter-ions surround the second monomers. These numbers actually correspond to the degrees of oxidation of the first and second patterns, respectively so that our overall simulation cell is neutral. If n_1 and n_2 both equal 2, the polymer is unloaded. If $n_1 = n_2 = 3$, the polymer is fully loaded. With these notations, a dimer will be denoted :



At the cathode,



At the anode,



So that the Gibbs free energy of the balanced equation reads,

$$\Delta G = G^{D2,2} + G_0 - G^{D3,3}$$

where the total energy corresponding to LiCl – Li(bcc) is noted G_0 . $G^{D2,2}$ and $G^{D3,3}$

are the total energy of the dimers obtained by the DFT calculation. The corresponding voltage is

$$\text{calculated by forming: } V = -(G^{D2,2} + 2G_0 - G^{D3,3})/2F$$

- **Calculated interatomic distances**

Here, we present the interatomic distances as obtained by our First Principles calculations, defining the local geometry all around Fe sites. **Table S.1** focuses on the effects induced by the introduction of counter-ions while **Table S.2** displays the differences caused by the nature of these counter-ions between each other's.

Table S.1. Selected calculated bond lengths for $[M(\text{bPy})_3]^{2+}$ and $[M(\text{bPy})_3]^{3+}$ complex when considered alone and in the field created by the PF_6^- counter-ions. They are compared to the experimental values reported into bracket (extracted from references⁷⁻¹⁰). All bond lengths are given in Å.

	$[\text{Fe}(\text{DmbPy})_3]^{2+}$		$[\text{Fe}(\text{DmbPy})_3]^{3+}$	
	alone	in 2 PF_6^- field	alone	in 3 PF_6^- field
Fe-N	1.96 [1.965]	1.960 [1.965]	1.98 [1.96]	1.971 [1.96]
C₁-C₁'	1.470 [1.473]	1.468 [1.472]	1.471 [1.472]	1.465 [1.473]
N-C₁	1.363 [1.350]	1.371 [1.350]	1.370 [1.350]	1.369 [1.350]

Table S.2. Selected calculated bond lengths for $[M(\text{bPy})_3]^{2+}$ and $[M(\text{bPy})_3]^{3+}$ complex in the field created by the $\text{Ci} = \text{ClO}_4^-$, PF_6^- and TFSI^- counter-ions. X1, X2 and X3 stand for the center of mass of the three Ci surrounding the complex. All bond lengths are given in Å.

Ci	$[\text{Fe}(\text{DmbPy})_3]^{2+}/2\text{Ci}^-$			$[\text{Fe}(\text{DmbPy})_3]^{3+}/3\text{Ci}^-$		
	ClO_4^-	PF_6^-	TFSI^-	ClO_4^-	PF_6^-	TFSI^-
Fe-N	1.960	1.960	1.959	1.966	1.971	1.967
Fe- X1	5.948	6.263	5.508	5.234	5.388	5.303
Fe- X2	6.211	6.154	5.518	5.195	6.188	5.313
Fe- X3	-	-	-	5.129	5.821	5.274

- **Supplementary references**

- (1) Frisch; Trucks, G.; Schlegel, H.; Scuseria, G.; Robb, M.; Cheeseman, J.; Scalmani, G.; Barone, V.; Mennucci, B.; Petersson, G.; et al. Gaussian 09, Revision D.01. *Gaussian 09, Revision B.01, Gaussian, Inc., Wallingford CT*. 2016.
- (2) Kohn, W.; Sham, L. J. Self-Consistent Equations Including Exchange and Correlation Effects. *Phys. Rev.* **1965**, *140* (4A), A1133–A1138.
- (3) Weigend, F.; Ahlrichs, R. Balanced Basis Sets of Split Valence, Triple Zeta Valence and Quadruple Zeta Valence Quality for H to Rn: Design and Assessment of Accuracy. *Phys. Chem. Chem. Phys.* **2005**, *7* (18), 3297.
- (4) Weigend, F. Accurate Coulomb-Fitting Basis Sets for H to Rn. *Phys. Chem. Chem. Phys.*

2006, 8 (9), 1057.

- (5) Perdew, J. P.; Burke, K.; Ernzerhof, M. Generalized Gradient Approximation Made Simple. *Phys. Rev. Lett.* **1996**, 77 (18), 3865–3868.
- (6) Ernzerhof, M.; Scuseria, G. E. Assessment of the Perdew–Burke–Ernzerhof Exchange–Correlation Functional. *J. Chem. Phys.* **1999**, 110 (11), 5029–5036.
- (7) Scarborough, C. C.; Wieghardt, K. Electronic Structure of 2,2'-Bipyridine Organotransition-Metal Complexes. Establishing the Ligand Oxidation Level by Density Functional Theoretical Calculations. *Inorg. Chem.* **2011**, 50 (20), 9773–9793.
- (8) England, J.; Scarborough, C. C.; Weyhermüller, T.; Sproules, S.; Wieghardt, K. Electronic Structures of the Electron Transfer Series $[M(\text{Bpy})_3]^{n+}$, $[M(\text{Tpy})_2]^{n+}$, and $[\text{Fe}(\text{t Bpy})_3]^{n+}$ ($M = \text{Fe}, \text{Ru}$; $n = 3+, 2+, 1+, 0, 1-$): A Mössbauer Spectroscopic and DFT Study. *Eur. J. Inorg. Chem.* **2012**, 2012 (29), 4605–4621.
- (9) Batten, S. R.; Murray, K. S.; Sinclair, N. J. Tris(2,2'-Bipyridyl- N,N')Iron(II) Diperchlorate. *Acta Crystallogr. Sect. C Cryst. Struct. Commun.* **2000**, 56 (8), e320–e320.
- (10) Figgis, B.; Skelton, B.; White, A. Crystal Structure and E.S.R. of 2,2'-Bipyridylum Tris(2,2'-Bipyridyl)Iron(III) Tetraaperchlorate. *Aust. J. Chem.* **1978**, 31 (1), 57.